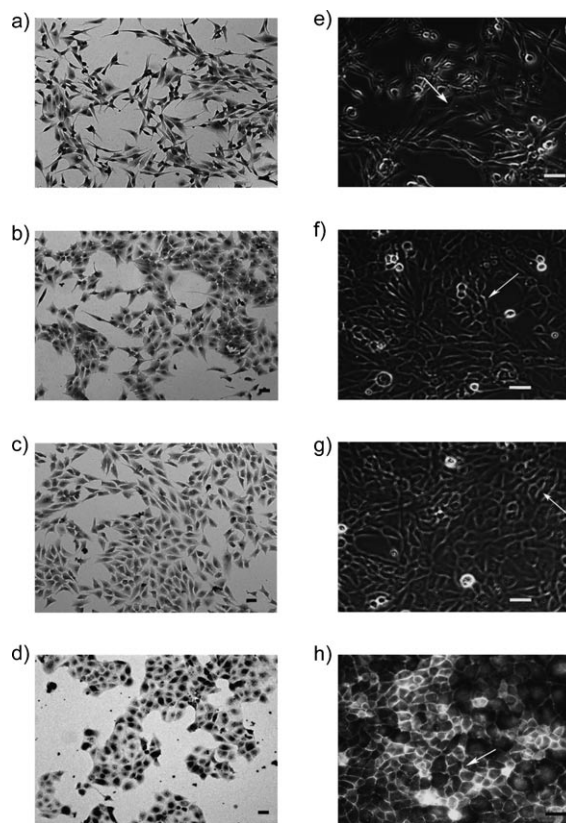


# The Ras Pathway Modulator Melophlin A Targets Dynamins\*\*

Tanja Knoth, Karin Warburg, Catherine Katzka, Amrita Rai, Alexander Wolf, Andreas Brockmeyer, Petra Janning, Thomas F. Reubold, Susanne Eschenburg, Dietmar J. Manstein, Katja Hübel, Markus Kaiser, and Herbert Waldmann\*

The Ras/mitogen-activated protein (MAP) kinase signal transduction pathway regulates numerous biological programs including cell growth and differentiation,<sup>[1,2]</sup> and harbors several important anticancer-drug targets.<sup>[3]</sup> Recent research, in particular inspired by systems biology approaches, revealed the importance of dynamic spatiotemporal regulation of and interplay between the Ras network members and their interaction with other signaling modules for fully functional Ras signaling.<sup>[4]</sup> Because of their rapid, conditional, and reversible mode of action, small-molecule modulators of protein function are particularly suitable tools for the conditional analysis of such dynamic biological processes, and hold great promise for the study of biological systems.<sup>[5]</sup> Therefore, the identification of novel small-molecule modulators of signaling through the Ras network and the identification of their molecular targets are of major interest.<sup>[1,3,6]</sup> The naturally occurring tetramic acids melophlin A and B (**1** and **2**, Scheme 1 A) reverse the morphology of H-Ras-transformed NIH3T3 fibroblasts at a concentration of  $5 \mu\text{g mL}^{-1}$  (that is,  $\text{IC}_{50} = 14 \mu\text{M}$ ).<sup>[7]</sup> However, the biological targets of the melophlins and their link to the Ras network have not been identified. Herein, we report the synthesis of a melophlin-inspired compound collection<sup>[8]</sup> and a subsequent chemical proteomics investigation, which revealed that melo-



**Figure 1.** Results of the phenotypic MDCK/MDCK-F3 cell assay. MDCK cells show a large and round phenotype and grow in a monolayer with cell-to-cell contacts. MDCK-F3 cells are long and spindle-like without regular cell-to-cell contacts, grow in multiple layers, and display impaired contact inhibition as demonstrated by the loss of E-cadherin expression on the cell surface. Cellular morphology was visualized microscopically by staining with Celestine blue (scale bars:  $19 \mu\text{m}$ ). a) MDCK-F3 cells (treated with dimethyl sulfoxide (DMSO) as negative control) show spindle-like morphology and do not form cell-to-cell contacts. b) MDCK-F3 cells show reversion of the phenotype after treatment with the MEK inhibitor U0126 at  $20 \mu\text{M}$  concentration. c) MDCK-F3 cells after treatment with melophlin A (**1**) at  $30 \mu\text{M}$  concentration. The cells display a round morphology comparable to the phenotype induced by treatment with U0126 and form cell-to-cell contacts. d) Wild-type MDCK cells show a round morphology and good cell-to-cell contacts. e) Fluorescein isothiocyanate (FITC) anti-E-cadherin staining of MDCK-F3 cells (treated with DMSO as negative control). Cells do not show cell-to-cell contacts, therefore E-cadherin is not enriched at the cell interfaces. f) E-cadherin immunostaining of MDCK-F3 cells. The arrow points to restored E-cadherin expression at the cell/cell interfaces after treatment with  $20 \mu\text{M}$  U0126. g) E-cadherin staining of MDCK-F3 cells treated with  $50 \mu\text{M}$  melophlin A (**1**). The arrow points to an example for restoration of E-cadherin expression at cell/cell interfaces. h) E-cadherin immunostaining of wild-type MDCK cells. E-cadherin immunostaining at the interfaces shows strong cell-to-cell contact formation.

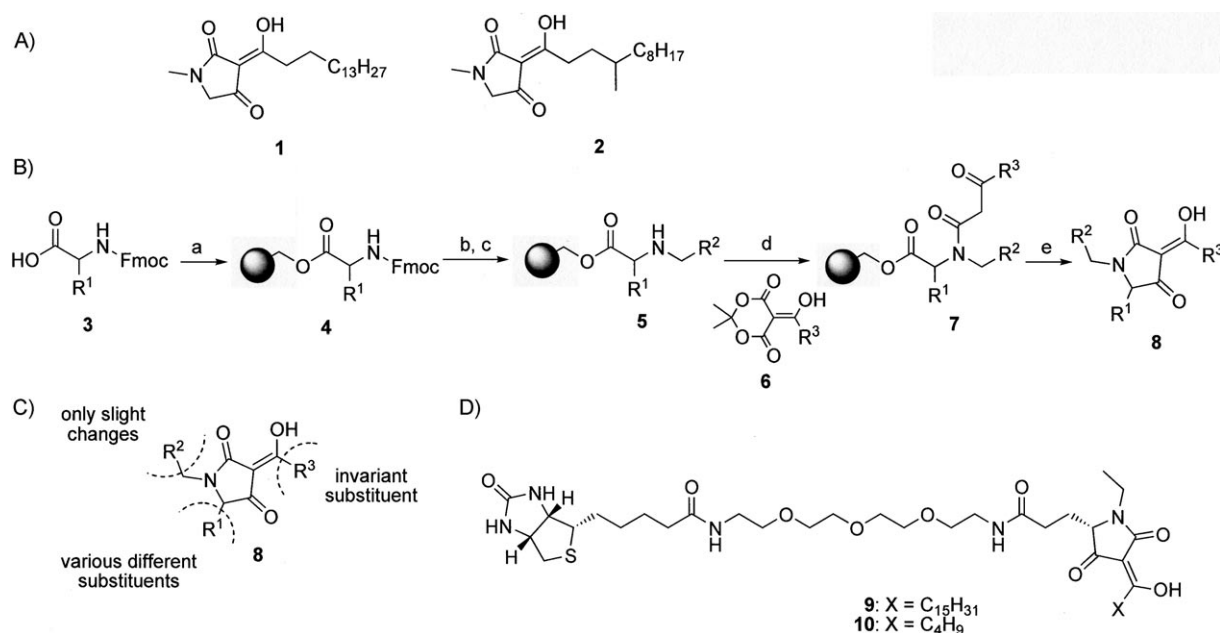
[\*] Dr. T. Knoth, Dipl.-Biol. K. Warburg, Dr. C. Katzka, Dr. A. Wolf, Dipl.-Ing. (FH) A. Brockmeyer, Dr. P. Janning, Dr. K. Hübel, Prof. Dr. H. Waldmann  
Max-Planck-Institut für molekulare Physiologie  
Abt. Chemische Biologie  
Otto-Hahn-Straße 11, 44227 Dortmund (Germany)  
and  
Technische Universität Dortmund  
Fakultät Chemie, Chemische Biologie  
Fax: (+49) 231-133-2499  
E-mail: herbert.waldmann@mpi-dortmund.mpg.de

Dr. T. F. Reubold, Dr. S. Eschenburg  
Max-Planck-Institut für molekulare Physiologie  
Abt. Strukturbiochemie, Dortmund (Germany)  
M.Sc. A. Rai, Prof. Dr. D. J. Manstein  
Medizinische Hochschule Hannover, Zentrum Biochemie  
Institut für Biophysikalische Chemie, Hannover (Germany)

Dr. M. Kaiser  
Chemical Genomics Centre der Max-Planck-Gesellschaft, Dortmund (Germany)

[\*\*] This research was supported by the Max-Planck-Gesellschaft, Deutsche Forschungsgemeinschaft (MA 1081/7-2) (D.J.M.), and the Fonds der Chemischen Industrie (H.W., D.J.M.).

Supporting information for this article is available on the WWW under <http://dx.doi.org/10.1002/anie.200902023>.



**Scheme 1.** A) Structures of melophlin A (1) and B (2). B) Synthesis of the tetramic acid collection and design of an affinity pull-down reagent based on structure–activity correlation. Conditions: a) *N,N'*-diisopropylcarbodiimide, CH<sub>2</sub>Cl<sub>2</sub>, DMF, 0 °C, 0.5 h; then Wang resin, DMAP, DMF, RT, 8 h; Fmoc = 9-fluorenylmethoxycarbonyl, DMF = dimethylformamide, DMAP = 4-dimethylaminopyridine; b) two times DMF/piperidine 4:1, RT, 15 min; c) R<sup>2</sup>CHO, THF, NaB(OAc)<sub>3</sub>H, NaOAc, RT, 12 h; d) acyl Meldrum's acid 6, toluene, 80 °C, 3 h; e) KOH (0.1 M in methanol), dioxane/CH<sub>2</sub>Cl<sub>2</sub>, RT, 3 h. Overall yield 5–83 %. C) Structure–activity relationship deduced from the Ras reporter gene assay for compounds active up to a concentration of 30  $\mu$ M, which are not toxic in this concentration range. D) Chemical structures of the biotinylated affinity probes 9 (active and nontoxic analogue of melophlin A) and 10 (inactive and nontoxic negative control probe).

phlin A unexpectedly targets dynamins in cells and thereby modulates signal transduction through the Ras network.

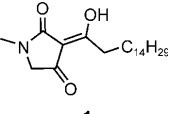
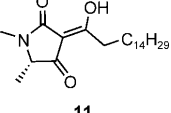
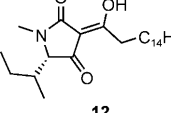
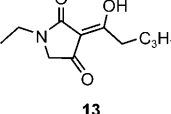
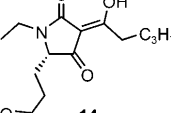
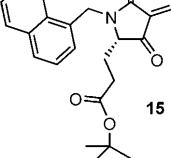
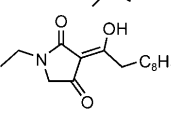
To strengthen the link between melophlin A and Ras signaling, we synthesized the natural product (see below) and subjected it to a PathDetect reporter gene assay (Stratagene), which quantifies Ras/MAP kinase signaling, and a WST-1 proliferation assay (see the Supporting Information).<sup>[9]</sup> Melophlin A inhibited the reporter signal with an IC<sub>50</sub> value of (18.1  $\pm$  1.2)  $\mu$ M and was not cytotoxic to the employed cell line up to a concentration of 30  $\mu$ M. In addition, melophlin A was investigated in a phenotype-based assay using epithelial Madine–Darby canine kidney (MDCK) cells and MDCK-F3 cells, which are MDCK cells transfected with the constitutively active H-RasG12V oncogene (Figure 1).<sup>[10]</sup> Since the H-Ras oncogene is the effector of the typical visible morphological differences between these cell lines, quantification of the phenotypic reversion of H-Ras-transformed cells can be used to measure the potency of small-molecule inhibitors of the activated H-Ras pathway.<sup>[6,11]</sup>

Treatment of MDCK-F3 cells with melophlin A at the noncytotoxic concentration of 30  $\mu$ M (see the Supporting Information and Table 1) caused reversal to the phenotype that is characteristic for untransformed MDCK cells (Figure 1). A comparable phenotypic reversal was induced by the Ras pathway (MEK) inhibitor U0126<sup>[12]</sup> (Figure 1). To correlate the activity of melophlin A with its chemical structure, we synthesized a focused collection of 60 melophlin analogues on the solid phase by following established methods<sup>[13]</sup> (Scheme 1B; for a list of all synthesized analogues, see the Supporting Information). To this end, Wang

resin was loaded by means of Steglich esterification with various Fmoc-protected amino acids containing aliphatic, benzylic, polar, acidic, or basic side-chain residues. After removal of the Fmoc protecting group, the liberated amino group was subjected to reductive amination with different aliphatic, benzylic, or alkenyl aldehydes. Treatment of the resulting secondary amines 5 with acyl Meldrum's acid 6 embodying alkyl, cycloalkyl, alkenyl, and aromatic residues gave the intermediate  $\beta$ -ketoamides 7 which, upon treatment with 0.1 M KOH, were cyclized with simultaneous release of the desired tetramic acid potassium salts from the polymeric carrier. If required, additional amino acid side-chain protecting groups were removed before melophlin A-derived tetramic acids were purified to homogeneity by reversed-phase HPLC (RP-HPLC) and finally obtained in 5–83 % overall yield. These compounds were then subjected to the assays described above. Noncytotoxic compounds that induced both phenotype reversal in MDCK-F3 cells and more than 30 % inhibition of the signal in the reporter gene assay at 30  $\mu$ M concentration were considered as hits. These criteria were met by only three compounds including melophlin A (Table 1 and Supporting Information).

For activity in the phenotypic screen, variation of the substituent at C5 is tolerated. Increasing the size of the nitrogen substituent beyond an ethyl group and even moderate shortening of the tetramic acid side chain at C3 drastically reduce the phenotype reversion (Scheme 1C; see also the Supporting Information). Based on these results, compound 9 (Scheme 1D), which incorporates a glutamic acid side chain and an alkyl chain of the same length as in the

**Table 1:** Results of the phenotype and reporter gene assay and determination of cytotoxicity. Data for melophlin A (**1**) are shown for comparison.

Compound	Phenotype ED <sub>50</sub> MDCK- F3 [ $\mu\text{M}$ ] <sup>[a]</sup>	Cytotoxicity LD <sub>25</sub> MDCK- F3 [ $\mu\text{M}$ ] <sup>[b]</sup>	Reporter gene assay IC <sub>50</sub> HLR [ $\mu\text{M}$ ] <sup>[c]</sup>	Cytotoxicity LD <sub>25</sub> HLR [ $\mu\text{M}$ ] <sup>[d]</sup>
 <b>1</b>	30	50	18.1 $\pm$ 1.2	30
 <b>11</b>	20	30	16.8 $\pm$ 3.4	30
 <b>12</b>	20	30	30 $\pm$ 2.5	30
 <b>13</b>	no effect	50	no effect	30
 <b>14</b>	no effect	50	no effect	30
 <b>15</b>	no effect	50	36.5 $\pm$ 5	30
 <b>16</b>	no effect	30	23.8 $\pm$ 0.8	30
<b>9</b>	no effect	30	25.7 $\pm$ 2.9	30
<b>10</b>	no effect	50	no effect	30

[a] Concentration at which 50% of the MDCK-F3 cells show the reversed phenotype. [b] Concentration at which the number of living MDCK-F3 cells is reduced by 25%. All compounds were initially tested at 50  $\mu\text{M}$  concentration. If no toxicity was observed at the highest tested concentration, this concentration is given as LD<sub>25</sub>. [c] IC<sub>50</sub> value for inhibition of luciferase activity in a reporter gene assay (PathDetect from Stratagene) in HLR cells. All compounds were initially tested at 30  $\mu\text{M}$  concentration. [d] Concentration at which the number of living HLR cells was reduced by 25%. All compounds were initially tested at 30  $\mu\text{M}$  concentration. If no cytotoxicity was observed at the highest concentration tested, this is given as LD<sub>25</sub>.

guiding natural product, was synthesized and employed in affinity pull-down experiments from cell lysate to identify potential target protein(s) of melophlin A. Compound **10** (Scheme 1D), with a much shorter alkyl chain, was designed as inactive control molecule (for the synthesis of **9** and **10**, see the Supporting Information). Affinity pull-down reagent **9** was active in the reporter gene assay [IC<sub>50</sub> = (25.7  $\pm$  2.9)  $\mu\text{M}$ ] and was noncytotoxic up to 30  $\mu\text{M}$  concentration, whereas control compound **10** did not display any activity in the reporter gene assay.

Both biotinylated probes were immobilized on magnetic streptavidin-coated beads and incubated with HeLa cell lysates. Bound proteins were released by heating, separated by SDS-PAGE, and visualized by Coomassie staining. The proteins were identified by in-gel tryptic digest, separation of the resulting peptides by nano-RP-HPLC, and online mass spectrometry (MS) followed by MS/MS analysis (see the Supporting Information). Only proteins that were identified in the affinity chromatography experiment with active probe **9** but not with the inactive compound **10**, and that were identified in at least three out of four pull-down experiments, were considered potential targets.

By means of this method, dynamin II, dynamin I-like protein, and p120 catenin were identified as potential targets with relevance to Ras signaling. The sequence coverages for the proteins were approximately 6% for p120 catenin, 13% for dynamin II, and 8% for dynamin I-like protein. The identities of dynamin II and p120 catenin were confirmed by Western blotting with specific antibodies, which also revealed that the proteins were not bound by the control probe **10** (Figure 2).

p120 Catenin has been linked to the Ras pathway only indirectly through its putative role as binding partner of E-cadherins, regulating their expression level, and an associated change of the endothelial to the mesenchymal cellular phenotype, but little is known about the relevance of this finding.<sup>[14]</sup> However, the observed binding of melophlin A to dynamins is particularly interesting. Dynamins are GTPases (GTP = guanosine-5'-tri-

phosphate) involved in many processes including budding of transport vesicles, division of organelles, and cytokinesis,<sup>[15–19]</sup> and they hold a prominent role in endocytosis.<sup>[15,16]</sup> Endocytosis is required for full activation of MAP kinase (ERK) by growth factor receptors.<sup>[17]</sup> Dominant negative interfering dynamin mutants inhibit endocytosis and EGF- and insulin-stimulated ERK activation without interfering with Ras, Raf-1, and MAP kinase kinase (MEK) activity.<sup>[16,18]</sup> This finding led to the suggestion that after activation at the plasma

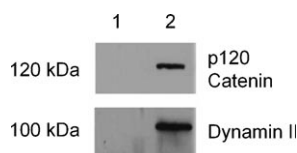


**Figure 2.** Identification of proteins isolated in the affinity pull-down experiment with the melophlin A-derived probe **9** and Western blot of resin-bound proteins. Proteins that were resolved by SDS-PAGE after affinity pull down were transferred to a nitrocellulose membrane and analyzed with specific antibodies. Lane 1 shows the control pull down with **10**, and lane 2 shows the pull down with active probe **9**. The cell lysates were analyzed with antibodies against the proteins p120 catenin and dynamin II. The results demonstrate that dynamin II and p120 catenin do not bind to negative control probe **10** but to active probe **9**.

membrane, MEK needs to traffic through the cytosol by means of the endocytotic pathway to fully activate ERK1/2.<sup>[19]</sup>

Decreased MAP kinase phosphorylation and activity upon inhibition of endocytosis by means of a dominant negative dynamin mutant has been shown in HeLa cells, that is, the model cell line investigated here.<sup>[18]</sup> To determine whether by analogy treatment of HeLa cells with melophlin A also leads to reduced MAP kinase phosphorylation, activation of MAP kinase (ERK1/ERK2) was investigated. As shown in Figure 3a, treatment of HeLa cells with 10  $\mu\text{M}$  melophlin A led to a decrease of ERK1/2 phosphorylation by 70% (for quantification, see Figure 6 in the Supporting Information).

Direct interaction of melophlin A with recombinantly produced human dynamin I-like protein, dynamin I, and dynamin II was monitored by surface plasmon resonance experiments with the biotinylated probe **9** immobilized on a Series S sensor chip SA. For full-length dynamin II, a dissociation constant  $K_d = (13.8 \pm 0.12) \mu\text{M}$  [ $k_{on} = (1.42 \times 10^3 \pm 1.54 \times 10^2) \text{M}^{-1} \text{s}^{-1}$ ,  $k_{off} = (1.95 \times 10^{-2} \pm 9.2 \times 10^{-3}) \text{s}^{-1}$ ] was determined (Figure 3b). Because of complex binding kinetics, the  $K_d$  values for dynamin I and dynamin I-like protein were calculated by direct measurement of the response at equilibrium for several concentrations.<sup>[20]</sup> The obtained data were analyzed by a sigmoidal equilibrium model and the  $K_d$  values were calculated to be  $K_d = (0.4 \pm 0.099) \mu\text{M}$  for dynamin I (1–760) and  $K_d = (0.6 \pm 0.042) \mu\text{M}$  for dynamin I-like protein (see also Figure 7 in the Supporting Information).

The dynamins embody a GTPase domain,<sup>[21]</sup> a middle domain, and a GTPase effector (GE) domain (Figure 3c). For dynamins I and II this basic set of domains is supplemented by two targeting domains, the pleckstrin homology (PH) domain and the proline-rich (PR) domain.<sup>[15]</sup> The truncated dynamin I (1–760) form employed here lacks the PR and the dynamin I-like protein used in our experiments does not possess the two targeting domains. Still, both proteins interact with melophlin A, which suggests that PH and PR are not crucial for the interaction.

To determine whether melophlin A acts as a GTPase inhibitor, the GTPase activity of dynamin II was monitored by using an enzyme-coupled continuous regenerative GTPase

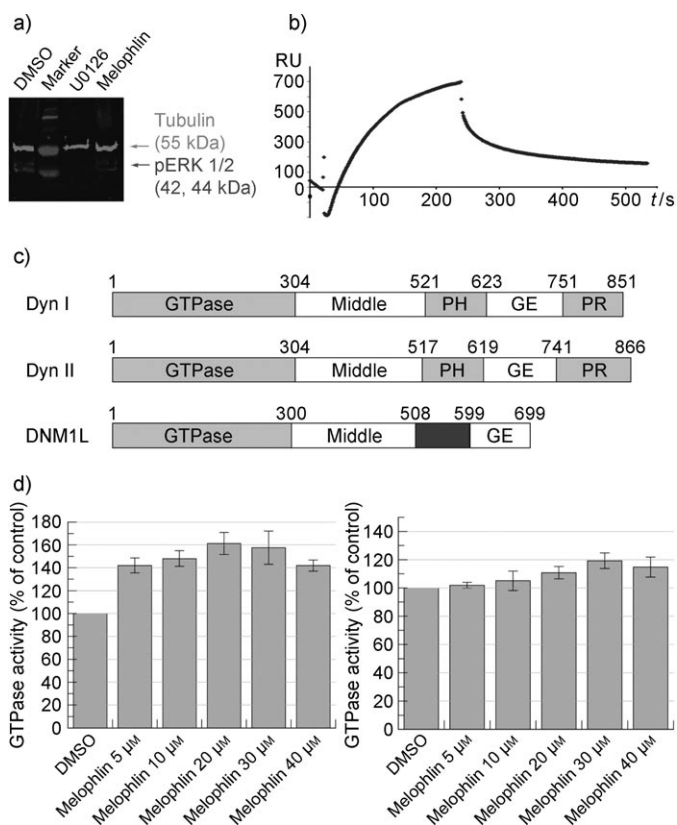


**Figure 3.** a) Representative Western blot showing reduced ERK phosphorylation in HeLa cells upon treatment with melophlin A. HeLa cells were treated with DMSO, melophlin A (10  $\mu\text{M}$ ), and the known MEK inhibitor U0126 (30  $\mu\text{M}$ ) overnight. After stimulation with EGF for 5 min the cells were lysed, and the lysate was separated by SDS-PAGE and subjected to immunoblotting for ERK. pERK1/2 as well as tubulin (as loading control) were detected with specific antibodies. Lane 1 shows the pERK signal after treatment of cells with DMSO. The signal is strongly reduced in lane 3, which shows reduction of ERK phosphorylation after treatment with U0126 (30  $\mu\text{M}$ ). In lane 4 only a weak pERK signal is visible, and shows reduction of ERK phosphorylation after incubation with melophlin A (10  $\mu\text{M}$ ). b) Binding of dynamin II to melophlin A determined by means of surface plasmon resonance. Melophlin A probe **9** was immobilized on the surface of a Series S sensor chip SA and binding to dynamin II was determined at a concentration of 3  $\mu\text{M}$ . The net binding curve is shown. Melophlin A analogue **9** binds dynamin II with  $K_d = (13.8 \pm 0.12) \mu\text{M}$ . c) Domain structure of dynamins. Domain boundaries are denoted by residue numbers. DNMI1L (dynamin I-like protein) contains an extra domain of unknown function between the middle domain and GED. d) Effect of melophlin A on the GTPase activity of full-length dynamin II (residues 1–866) at a concentration of 0.5  $\mu\text{M}$  (left panel) and effect of melophlin A on the GTPase activity of full-length dynamin II (residues 1–866) stimulated with GST-Grb2 at a concentration of 0.5  $\mu\text{M}$  (right panel). Measurements were done in triplicate; error bars are standard deviations.

assay, which revealed that melophlin A does not inhibit the GTPase activity of dynamin II in the presence or absence of Grb2. Rather, melophlin A slightly stimulates GTPase activity (Figure 3d).

To determine whether melophlin A interferes with endocytosis, internalization of the transferrin/transferrin receptor complex by means of receptor-mediated endocytosis was



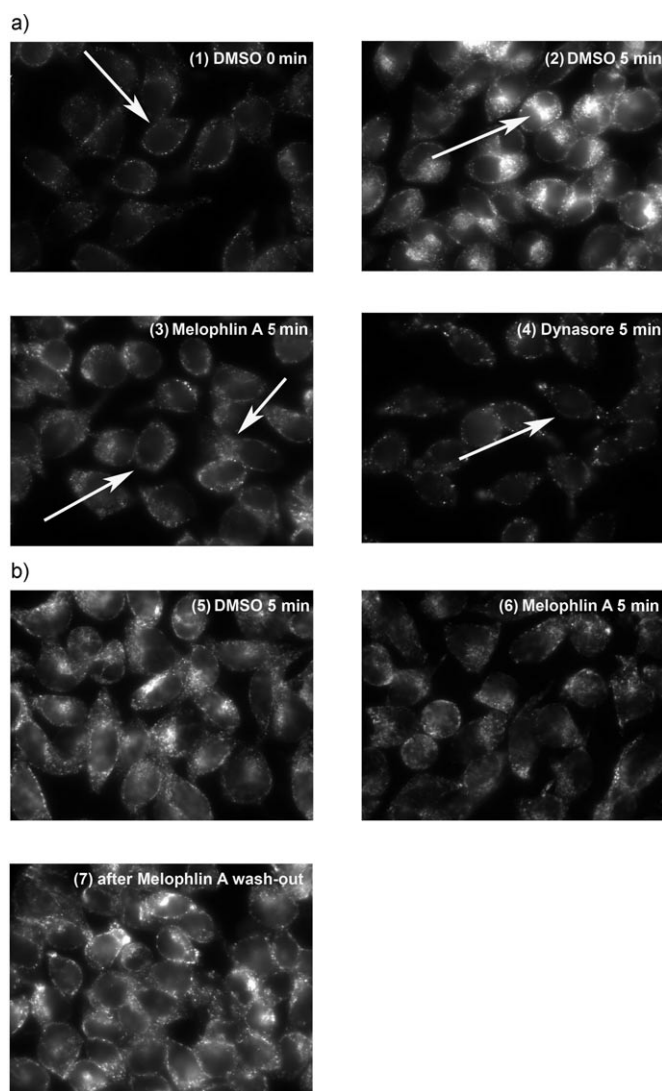


**Figure 4.** Inhibition of dynamin-dependent internalization of transferrin by melophlin. a) Alexa 546–transferrin was allowed to bind to the surface receptor of HeLa cells by incubation at 25 °C (time point 0 min (1)). Upon gentle heating to 37 °C, the bound transferrin was internalized. HeLa cells were incubated overnight at 37 °C in Dulbecco's modified Eagle's medium (DMEM) supplemented with 10% fetal calf serum (FCS) to confluency of about 50%. Medium was removed and cells were incubated for 3 h at 37 °C in DMEM without serum containing melophlin A (3; uptake of transferrin–Alexa is reduced in these cells; most of the transferrin is still localized at the cell surface (left arrow); only a little transferrin is internalized (right arrow)), dynasore (4, reduced transferrin uptake; transferrin is not internalized but still binds to the cell-surface receptors (arrow)), or 0.8% DMSO (2, the arrows point to transferrin taken up into the cells) as solvent control, followed by incubation for 2 min at room temperature in the same medium containing 25  $\mu\text{g mL}^{-1}$  transferrin–Alexa 546 (Invitrogen). Cells were washed three times with the same medium and incubated at 37 °C for 0 and 5 min, respectively, in the presence of inhibitors. Transferrin attached to the cell surface was removed by washing. Cells were fixed, mounted on cover slips, and imaged. b) Reversibility of the inhibition of transferrin internalization by melophlin A. The cells were incubated for 3 h at 37 °C with 25  $\mu\text{M}$  melophlin A (image 7) or 0.8% DMSO (image 5) in DMEM without serum. The cells were washed three times with the medium without inhibitor and incubated for 12 h at 37 °C with DMEM with 10% FCS. The positive control was incubated for the last 3 h in DMEM without serum in the presence of 25  $\mu\text{M}$  melophlin A (image 6). Transferrin internalization was visualized as described above. Image 5 shows internalization of transferrin in cells treated with DMSO. In cells pretreated with melophlin A (image 6) internalization is inhibited. After wash-out of the compound, the cells were allowed to recover. Recovered cells (image 7) show full restoration of transferrin–Alexa internalization, thus revealing that the effect is reversible.

monitored, which requires normal dynamin function.<sup>[22]</sup> As a positive control we used dynasore, the only known inhibitor, which interferes with endocytosis by noncompetitive inhibition of the GTPase activity of dynamin.<sup>[23]</sup> As shown in Figure 4, the uptake of transferrin was reduced to 30% after incubation with 20  $\mu\text{M}$  melophlin A for three hours. Uptake inhibition is dose-dependent (see Figure 8 in the Supporting Information) and can be reversed by wash-out of melophlin A and 12 hours of recovery without the compound. Note that at concentrations greater than 20  $\mu\text{M}$  the reduction of ERK phosphorylation and the inhibition of transferrin endocytosis decrease. This may be a result of aggregation of melophlin A in an aqueous environment at greater than or equal to 20  $\mu\text{M}$ , as indicated by dynamic light scattering experiments (see the Supporting Information) and the observed increase in GTPase stimulation by melophlin A at such concentrations (see above). These findings suggest that melophlin A should preferably be employed at concentrations up to about 20  $\mu\text{M}$  in biological experiments.

In the light of these results, the observed phenotypic effects induced by treatment with melophlin A are most likely

because of inhibition of receptor-mediated endocytosis. Melophlin A binds to dynamin II and dynamin I-like protein, that is, the mitochondrial homologue of dynamin in HeLa cells. Dynamin I is not expressed in these cells and consequently could not be identified in the affinity pull-down experiments. However, as shown in the surface plasmon resonance experiment, melophlin A binds dynamin I as well.

Our results identify melophlin A as a new modulator of dynamin activity that inhibits dynamin's functions by means of a yet unidentified mechanism, which differs from the mode of action of dynasore, the only other known dynamin inhibitor so far. We provide experimental proof that the previously described connection between dynamin-mediated endocytosis and Ras/MAP kinase signaling can be antagonized by small molecules. These insights will open up new opportunities for the study of the Ras/MAP kinase network and may provide new avenues for medicinal chemistry research.

Received: April 15, 2009

Revised: July 21, 2009

Published online: August 31, 2009

**Keywords:** biological activity · natural products · proteomics · solid-phase synthesis · structure–activity relationships

[1] A. Wittinghofer, H. Waldmann, *Angew. Chem.* **2000**, *112*, 4360–4383; *Angew. Chem. Int. Ed.* **2000**, *39*, 4192–4214.

- [2] W. Kolch, *Biochem. J.* **2000**, *351*, 289–305.
- [3] J. Downward, *Nat. Rev. Cancer* **2003**, *3*, 11–22.
- [4] a) O. Rocks, A. Peyker, M. Kahms, P. J. Verveer, C. Koerner, M. Lumbierres, J. Kuhlmann, H. Waldmann, A. Wittinghofer, P. I. H. Bastiaens, *Science* **2005**, *307*, 1746–1752; b) O. Rocks, A. Peyker, P. I. H. Bastiaens, *Curr. Opin. Cell Biol.* **2006**, *18*, 351–357; c) W. Kolch, *Nat. Rev. Mol. Cell Biol.* **2005**, *6*, 827–837.
- [5] a) D. P. Walsh, Y. T. Chang, *Chem. Rev.* **2006**, *106*, 2476–2530; b) J. Lehár, B. R. Stockwell, G. Giaever, C. Nislow, *Nat. Chem. Biol.* **2008**, *4*, 674–681.
- [6] H. Waldmann, I. M. Karaguni, M. Carpintero, E. Gourzoulidou, C. Herrmann, C. Brockmann, H. Oschkinat, O. Müller, *Angew. Chem.* **2004**, *116*, 460–464; *Angew. Chem. Int. Ed.* **2004**, *43*, 454–458.
- [7] S. Aoki, K. Higuchi, Y. Ye, R. Satari, M. Kobayashi, *Tetrahedron* **2000**, *56*, 1833–1836.
- [8] For previous syntheses of melophlins and for related compounds, see: a) R. Schobert, A. Schlenk, *Bioorg. Med. Chem.* **2008**, *16*, 4203–4221; b) R. Schobert, C. Jagusch, *Tetrahedron* **2005**, *61*, 2301–2307; c) C. Y. Wang, B. G. Wang, S. Wiryowidagdo, V. Wray, R. van Soest, K. G. Steube, H. S. Guan, P. Proksch, R. Ebel, *J. Nat. Prod.* **2003**, *66*, 51–56; d) J. Xu, M. Hasegawa, K. Harada, H. Kobayashi, H. Nagai, M. Namikoshi, *Chem. Pharm. Bull.* **2006**, *54*, 852–854; e) B. Biersack, R. Diestel, C. Jagusch, G. Rapp, F. Sasse, R. Schobert, *Chem. Biodiversity* **2008**, *5*, 2423–2430.
- [9] M. V. Berridge, A. S. Tan, *Arch. Biochem. Biophys.* **1993**, *303*, 474–482.
- [10] J. Behrens, M. M. Mareel, F. M. Van Roy, W. Birchmeier, *J. Cell Biol.* **1989**, *108*, 2435–2447.
- [11] a) C. Herrmann, C. Block, C. Geisen, K. Haas, C. Weber, G. Winde, T. Moroy, O. Müller, *Oncogene* **1998**, *17*, 1769–1776; b) I. M. Karaguni, P. Herter, P. Debruyne, S. Chtarbova, A. Kasprzynski, U. Herbrand, M. R. Ahmadian, K. H. Glusen-kamp, G. Winde, M. Mareel, T. Moroy, O. Müller, *Cancer Res.* **2002**, *62*, 1718–1723; c) O. Müller, E. Gourzoulidou, M. Carpintero, I. M. Karaguni, A. Langerak, C. Herrmann, T. Moroy, L. Klein-Hitpass, H. Waldmann, *Angew. Chem.* **2004**, *116*, 456–460; *Angew. Chem. Int. Ed.* **2004**, *43*, 450–454.
- [12] M. F. Favata, K. Y. Horiuchi, E. J. Manos, A. J. Daulerio, D. A. Stradley, W. S. Feeser, D. E. Van Dyk, W. J. Pitts, R. A. Earl, F. Hobbs, R. A. Copeland, R. L. Magolda, P. A. Scherle, J. M. Trzaskos, *J. Biol. Chem.* **1998**, *273*, 18623–18632.
- [13] a) T. T. Romoff, L. Ma, Y. W. Wang, D. A. Campbell, *Synlett* **1998**, 1341–1342; b) S. P. Raillard, W. W. Chen, E. Sullivan, W. Bajjalieh, A. Bhandari, T. A. Baer, *J. Comb. Chem.* **2002**, *4*, 470–474; c) U. S. Sørensen, E. Falch, P. Krogsgaard-Larsen, *J. Org. Chem.* **2000**, *65*, 1003–1007.
- [14] M. S. Kinch, G. J. Clark, C. J. Der, K. Burrige, *J. Cell Biol.* **1995**, *130*, 461–471.
- [15] G. J. K. Praefcke, H. T. McMahon, *Nat. Rev. Mol. Cell Biol.* **2004**, *5*, 133–147.
- [16] H. S. Shpetner, J. S. Herskovits, R. B. Vallee, *J. Biol. Chem.* **1996**, *271*, 13–16.
- [17] S. Roy, B. Wyse, J. F. Hancock, *Mol. Cell. Biol.* **2002**, *22*, 5128–5140.
- [18] A. V. Vieira, C. Lamaze, S. L. Schmid, *Science* **1996**, *274*, 2086–2089.
- [19] O. Kranenburg, I. Verlaan, W. H. Moolenaar, *J. Biol. Chem.* **1999**, *274*, 35301–35304.
- [20] J. E. Ladbury, M. A. Lemmon, M. Zhou, J. Green, M. C. Botfield, J. Schlessinger, *Proc. Natl. Acad. Sci. USA* **1995**, *92*, 3199–3203.
- [21] T. F. Reubold, S. Eschenburg, A. Becker, M. Leonard, S. L. Schmid, R. B. Vallee, F. J. Kull, D. J. Manstein, *Proc. Natl. Acad. Sci. USA* **2005**, *102*, 13093–13098.
- [22] M. Ehrlich, W. Boll, A. van Oijen, R. Hariharan, K. Chandran, M. L. Nibert, T. Kirchhausen, *Cell* **2004**, *118*, 591–605.
- [23] E. Macia, M. Ehrlich, R. Massol, E. Boucrot, C. Brunner, T. Kirchhausen, *Dev. Cell* **2006**, *10*, 839–850.